

## SO<sub>2</sub>-Induced Isomerization of 2-Butene over Cation-Exchanged X Zeolites

KIYOSHI OTSUKA AND AKIRA MORIKAWA

*Department of Chemical Engineering, Tokyo Institute of Technology,  
Ookayama, Meguro-ku, Tokyo 152, Japan*

Received October 25, 1977; revised June 14, 1978

SO<sub>2</sub> adsorbed on alkali-, alkaline earth-, and rare earth-exchanged X zeolites induces the isomerizations of *cis*-2-butene. Different kinetic behavior between the two isomerizations (*cis-trans* isomerization and double-bond migration) has suggested that the two isomerizations proceed via different mechanisms. The geometrical isomerization has been interpreted by means of the previously suggested mechanism where the *cis-trans* conversion is accompanied by the cooligomerization of SO<sub>2</sub> and 2-butene. Activities of the zeolites for this reaction have been correlated to the polarizing power of the exchangeable cation of the zeolites, suggesting that the initiation of the cooligomerization (and accordingly the geometrical isomerization) takes place by means of a polarization of the charge-transfer complex, formed from SO<sub>2</sub> and 2-butene, under the influence of metal cations. It is inferred that the SO<sub>2</sub>-induced double-bond migration observed on alkaline-earth and rare-earth zeolites is caused by the generation of new acidic OH groups through the reaction of SO<sub>2</sub> with basic OH groups bonded to metal cations.

### INTRODUCTION

Many studies have shown the effects of the favorable action of guest molecules on the rate of transformation of a reactant or reactants (1, 2). The promoting molecules are not reaction products and may not be converted into reaction products after a reaction has been completed on the catalyst. This effect of foreign molecules has been recognized specifically on zeolites with a few exceptions (3).

The activating action of SO<sub>2</sub> in hydrocarbon conversions, such as cracking, alkylation, or isomerization over X and Y zeolites, was first reported in patents over 10 years ago (4, 5). However, no detailed studies on this subject have been reported since. It was recently shown that SO<sub>2</sub> preadsorbed on various metal oxides or alkali cation-exchanged zeolites induces *cis-trans* isomerization of 2-butene without enhanc-

ing the rate of double-bond migration (6, 7). It was suggested that this selective isomerization occurs through the addition and elimination of butene molecules at the terminal of the polymer during the progress of the copolymerization of SO<sub>2</sub> and 2-butene (7, 8). Furthermore, it has been suggested that the charge-transfer complex of SO<sub>2</sub> and 2-butene participates in the initiation process of the copolymerization (9). However, how the complex initiates the polysulfone-accompanying isomerization is still obscure.

In the case of alkaline earth-, rare earth-, or transition metal cation-exchanged X zeolites, preliminary experiments showed that SO<sub>2</sub> causes not only geometrical isomerization but also double-bond migration of normal butenes at room temperature (10). It has been shown that the two isomerizations over ZnX zeolite take place

by means of different mechanisms over different active sites (10). However, detailed mechanisms and the nature of the active sites for the two reactions are not known.

In this work, the kinetic study of the effect of SO<sub>2</sub> on the isomerizations of *cis*-2-butene over alkali-, alkaline earth-, and rare earth-exchanged X zeolites has been carried out. The catalytic activities of these zeolites for the SO<sub>2</sub>-induced isomerizations have been examined in connection with the influence of exchangeable cations of zeolites. A possible scheme of the initiation step for the polysulfone-accompanying isomerization and the nature of the active sites for the two isomerizations (geometrical isomerization and double-bond migration) are discussed along with these results.

#### EXPERIMENTAL

The original NaX (13X from Linde; SiO<sub>2</sub>/Al<sub>2</sub>O<sub>3</sub> = 2.8; surface area, 678 m<sup>2</sup>/g) sample was exchanged with an NaCl solution to decrease impurity cation content. All forms of zeolites were prepared by conventional ion exchange of an NaX zeolite. The ion exchange was carried out at 25°C with a 0.5 *N* solution of the appropriate chlorides, where the mole ratio of exchangeable cations of liquid to those of solid applied during the exchange was 10. The degree of exchange was expressed by 100 ([Al] - [Na])/[Al], which was determined by atomic absorption of aluminum and residual sodium of the corresponding zeolite.

The apparatus employed was a conventional mercury-free gas circulating system with a 225-ml dead volume, capable of achieving a vacuum to 10<sup>-6</sup> Torr. Materials used and analysis of butene isomers have been described elsewhere (7).

Prior to every run, the catalyst (~0.05–0.10 g) in the reactor was calcined at 500°C in dried oxygen and degassed under vacuum for 2 hr at the same temperature. After the preadsorption of SO<sub>2</sub> at 25°C for 30 min,

the reaction was started at the same temperature by feeding *cis*-2-butene (1.29 × 10<sup>-3</sup> mol) and circulating the gas through the catalyst bed. A small amount of the reacting gases was periodically collected and analyzed by gas chromatography. The initial rates of the two isomerizations,  $R^0_{c \rightarrow t}$  (the rate of *trans*-2-butene formation) and  $R^0_{c \rightarrow 1}$  (the rate of 1-butene formation), are the average rates calculated from the concentration of *trans*-2- and 1-butene produced within 7 min. It was confirmed that the preadsorbed SO<sub>2</sub> does not desorb to gas phase until its amount reaches to about 2 × 10<sup>-3</sup> mol/g, which was checked by the analysis of SO<sub>2</sub> in gas phase during the progress of the reaction on NaX zeolite.

#### RESULTS

In the absence of SO<sub>2</sub>, the initial rates of two isomerizations of *cis*-2-butene for various cation-exchanged X zeolites have been measured at 25°C (Table 1). Alkali and alkaline earth zeolites did not show any catalytic activity for the reactions; rare earth zeolites have high catalytic activities.

When SO<sub>2</sub> is added onto the zeolites at 25°C, a considerable increase in the catalytic activities of the zeolites has been shown for every zeolite in Table 1.

##### *Alkali Cation-Exchanged Zeolite*

SO<sub>2</sub> adsorbed on LiX, NaX, and KX zeolites causes geometrical isomerization alone without accompanying any double-bond migration. The absence of the latter isomerization has been checked by using 1-butene as the starting olefin. SO<sub>2</sub>-induced isomerizations over RbX and CsX zeolites were too slow to be measured (<0.02 × 10<sup>-8</sup> mol·sec<sup>-1</sup>·g<sup>-1</sup>) at the concentration of SO<sub>2</sub> of 1.8 × 10<sup>-4</sup> mol/g. Examples of the fraction of *trans*-2-butene produced versus time for LiX, NaX, and KX are plotted in Fig. 1. In the case of LiX and

TABLE 1

Rates of the Two Isomerizations of *cis*-2-Butene in the Absence of SO<sub>2</sub> at 25°C

Zeolite	Percentage of cation exchanged	$R_{c \rightarrow t}^0 \times 10^8$ (mol·sec <sup>-1</sup> ·g <sup>-1</sup> )	$R_{c \rightarrow 1}^0 \times 10^8$ (mol·sec <sup>-1</sup> ·g <sup>-1</sup> )
LiX	60	n <sup>a</sup>	n
NaX	—	n	n
KX	79	n	n
RbX	61	n	n
CsX	64	n	n
MgX	76	n	n
CaX	83	n	n
SrX	94	n	n
BaX	81	n	n
LaX	83	4.22	7.58
CeX	84	57.5	22.2
NdX	87	6.78	11.3

<sup>a</sup> n represents a rate less than  $0.03 \times 10^{-8}$  mol·sec<sup>-1</sup>·g<sup>-1</sup>.

NaX, the rates of geometrical isomerization are accelerated with time.

The effect of the concentration of preadsorbed SO<sub>2</sub> on the initial rates of geometrical isomerization is indicated in Fig. 2. The rates are proportional to the amount of SO<sub>2</sub> when its concentration is low. However, the rate decreases under high concentration of SO<sub>2</sub> as can be seen in the case of NaX zeolite.<sup>1</sup>

#### Alkaline Earth Zeolites

Addition of SO<sub>2</sub> onto MgX, CaX, SrX, and BaX zeolites induces both reactions, i.e., geometrical isomerization and double-bond migration. Values of the fraction of products produced as a function of time are indicated in Fig. 3. Acceleration in the rate of geometrical isomerization with time can also be seen here. The effect of SO<sub>2</sub> is unusually greater on geometrical isomerization than on double-bond migration, which is demonstrated by extremely high ratios of the initial rates for the two isomerizations; i.e.,  $R_{c \rightarrow t}^0/R_{c \rightarrow 1}^0$  values are 437, 42.5,

<sup>1</sup> The NaX zeolite used in the previous work (7) has an activity about twice as high as that of the NaX in the present work. The higher activity of the former zeolite must be attributed to the presence of alkaline earth cations, probably Mg and Ca, as impurities because of the lack of exchange treatment in NaCl solution before use.

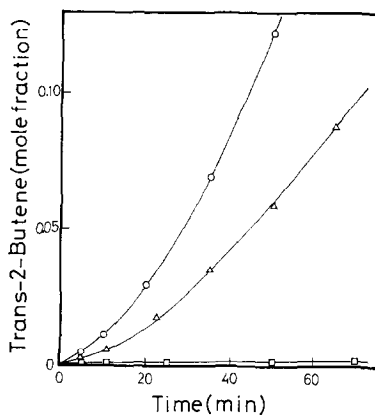


FIG. 1. Time dependence of the mole fraction of *trans*-2-butene produced on alkali zeolites: The reaction was carried out at 25°C using 0.10 g of the zeolite. ○, LiX (amount of SO<sub>2</sub> preadsorbed =  $1.75 \times 10^{-4}$  mol/g); △, NaX ( $1.58 \times 10^{-4}$  mol/g); □, KX ( $1.69 \times 10^{-4}$  mol/g).

23.8, and 143 for MgX, CaX, SrX, and BaX, respectively.

The effects of concentration of SO<sub>2</sub> on the initial rates of both isomerizations are shown in Figs. 4a-d for the four alkaline earth zeolites. The rate of geometrical isomerization increases proportionally with a rise in the amount of SO<sub>2</sub> within the range of the latter up to about  $2.2 \times 10^{-4}$  mol/g

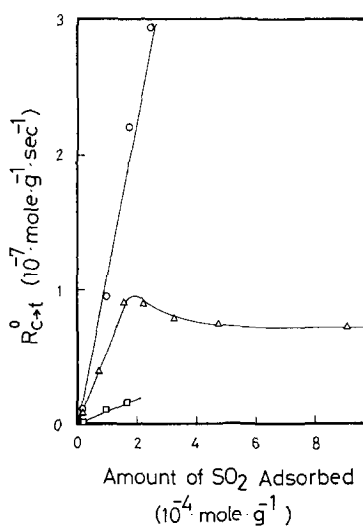


FIG. 2. Rate of SO<sub>2</sub>-induced geometrical isomerization as a function of the amount of SO<sub>2</sub> preadsorbed (alkali zeolites): ○, LiX; △, NaX; □, KX.

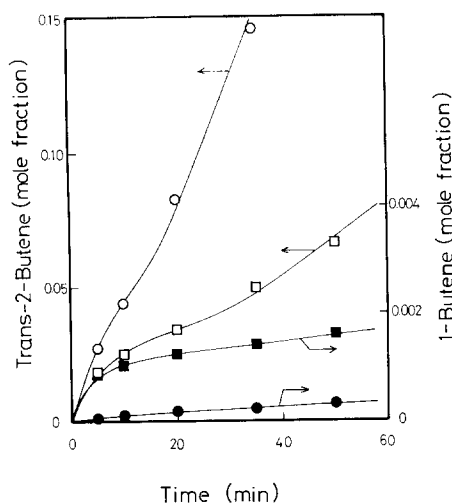


FIG. 3. Time dependence of the mole fraction of *trans*-2-butene and of 1-butene on alkaline earth zeolites: The reactions were carried out at 25°C. Weight of zeolites was 0.100 g. Amount of SO<sub>2</sub> preadsorbed was  $1.70 \times 10^{-4}$  mol/g for each zeolite. ○, MgX (*cis* → *trans*); ●, MgX (*cis* → 1), □, SrX (*cis* → *trans*); ■, SrX (*cis* → 1).

for every alkaline earth zeolite. At high concentration of SO<sub>2</sub>, however, the rate decreases with the amount of SO<sub>2</sub> as shown in the case of MgX. The rate of double-bond migration depends on the amount of adsorbed SO<sub>2</sub> in a quite different way from that for the rate of *cis*-*trans* isomerization as is demonstrated in the case of MgX and SrX. At a low concentration of SO<sub>2</sub>, it can be assumed for the alkaline earth zeolites examined here, except SrX, that the rate of double-bond migration is proportional to the amount of adsorbed SO<sub>2</sub>.

#### Rare Earth Zeolites

SO<sub>2</sub> preadsorbed on LaX, CeX, and NdX zeolites greatly enhances the rate of two isomerizations of *cis*-2-butene. The mole fraction of the products versus time plots for the two reactions are shown in Fig. 5. The rate of *trans*-2-butene formation is very fast at the earlier stage of the reaction, but it decreases sharply with reaction time. On the other hand, the rate of 1-butene formation does not change with time as

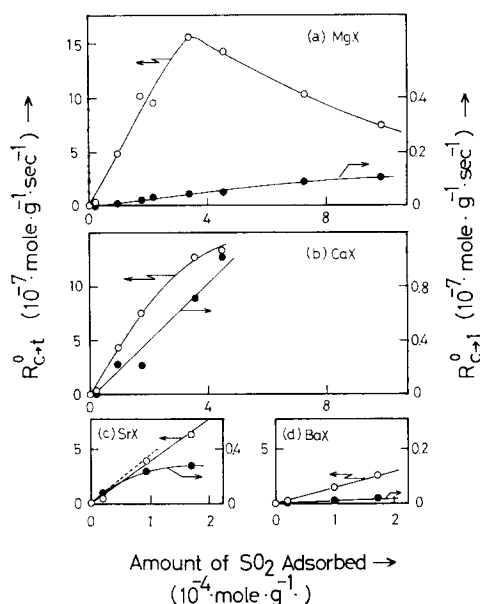


FIG. 4. Rate of SO<sub>2</sub>-induced isomerization as a function of the amount of SO<sub>2</sub> preadsorbed (alkaline earth zeolites): ○,  $R_{c \rightarrow t}^0$ ; ●,  $R_{c \rightarrow 1}^0$ . Activity of SrX in double-bond migration was estimated from the slope of the dotted line in (c).

much as that of geometrical isomerization does in the range of 5 to 60 min. Figure 6 shows the selectivity of geometrical isomer-

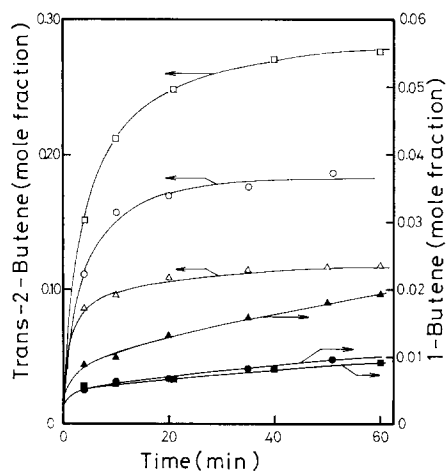


FIG. 5. Time dependence of the mole fraction of *trans*-2-butene and of 1-butene produced on rare earth zeolites: The reactions were carried out at 25°C. Weight of zeolites used was 0.100 g. Amount of SO<sub>2</sub> preadsorbed was  $(1.75 \pm 0.04) \times 10^{-4}$  mol/g. Open symbols,  $R_{c \rightarrow t}^0$ ; closed symbols,  $R_{c \rightarrow 1}^0$ . □ and ■, LaX; △ and ▲, CeX; ○ and ●, NdX.

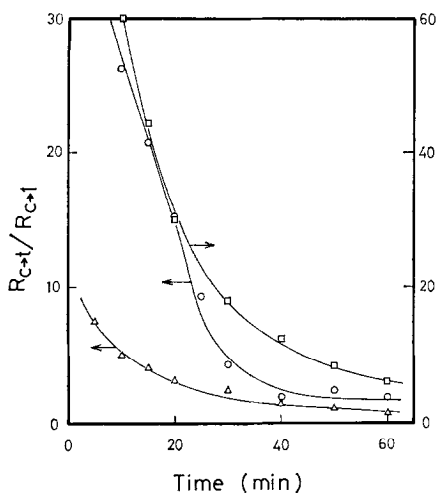


Fig. 6. Selectivity of geometrical isomerization as a function of time:  $\square$ , LaX;  $\circ$ , NdX;  $\triangle$ , CeX.

ization as a function of reaction time; where the selectivity was expressed by  $R_{c \rightarrow t}/R_{c \rightarrow 1}$ , the rates were estimated from the slopes of the curves in Fig. 5. The selectivities for the three rare earth zeolites decrease sharply with time until about 40 min, then the change becomes slow. High selectivities for geometrical isomerization and their unusual change with time (Fig. 6)

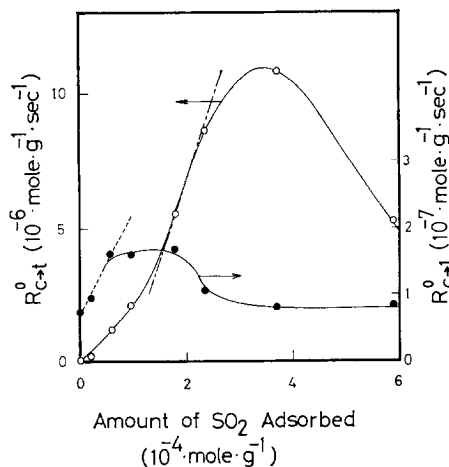


Fig. 7. Rates of the two isomerizations as a function of the amount of  $\text{SO}_2$  preadsorbed (LaX):  $\circ$ ,  $R_{c \rightarrow t}^0$ ;  $\bullet$ ,  $R_{c \rightarrow 1}^0$ . The slopes of the lines (---, geometrical isomerization; ----, double-bond migration) were applied for activity calculation (see text).

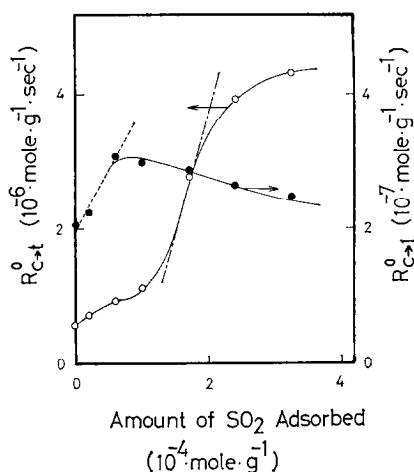


Fig. 8. Rates of the two isomerizations as a function of the amount of  $\text{SO}_2$  preadsorbed (CeX):  $\circ$ ,  $R_{c \rightarrow t}^0$ ;  $\bullet$ ,  $R_{c \rightarrow 1}^0$ .

are contrasted with the result obtained in the absence of  $\text{SO}_2$  that the selectivities for LaX, CeX and NdX lie in the range of 0.9 to 0.6 at the reaction times greater than 7 min.

The plots of initial rates of both isomerizations as a function of the amount of  $\text{SO}_2$  are illustrated in Figs. 7–9. The rates of geometrical isomerization for LaX and NdX increase with a rise in the amount of preadsorbed  $\text{SO}_2$  showing a greater than

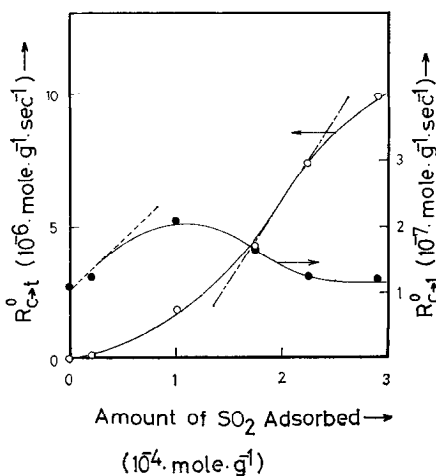


Fig. 9. Rates of the two isomerizations as a function of the amount of  $\text{SO}_2$  preadsorbed (NdX):  $\circ$ ,  $R_{c \rightarrow t}^0$ ;  $\bullet$ ,  $R_{c \rightarrow 1}^0$ .

first-order dependence on it, but similar to the results obtained with NaX and MgX, the rates show a tendency to decrease at high concentrations of SO<sub>2</sub>. Figures 7-9 show that the dependence of the rate of double-bond migration on the amount of SO<sub>2</sub> is quite different from that of geometrical isomerization;  $R_{c \rightarrow 1}^0$  reaches its maximum when the amount of SO<sub>2</sub> is about  $1 \times 10^{-4}$  mol/g and decreases with a rise in the amount of SO<sub>2</sub> while  $R_{c \rightarrow t}^0$  still increases sharply.

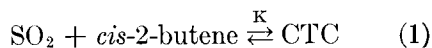
#### DISCUSSION

The unusually high selectivity of geometrical isomerization observed with every zeolite used in the present work and the very different dependences of the rates of two isomerizations on the amount of adsorbed SO<sub>2</sub> show that the two isomerizations induced by SO<sub>2</sub> occur via different mechanisms. This is supported by the quite different time dependency of the rates between the two isomerizations. A similar conclusion was also obtained with ZnX zeolite by examining the effect of reaction temperature or of pretreatment temperature on the rates of SO<sub>2</sub>-induced isomerizations (10).

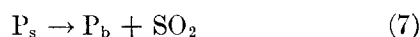
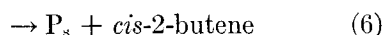
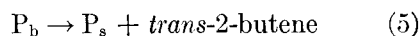
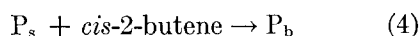
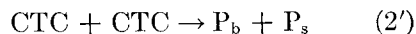
#### *cis-trans Isomerization*

The following reaction mechanism for the selective *cis-trans* isomerization induced

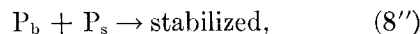
by SO<sub>2</sub> adsorbed over solid catalysts was suggested in the previous paper (7-9):



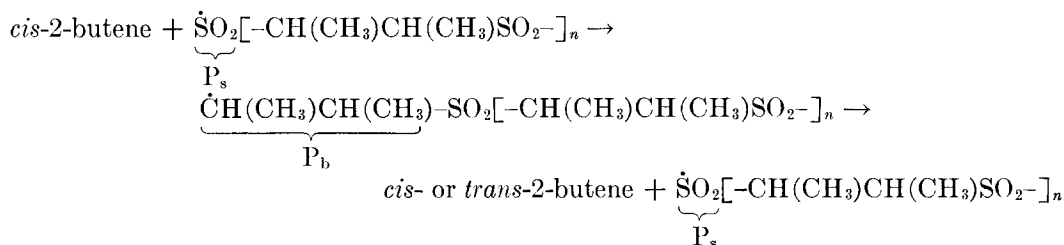
or



or



where the mechanism is considered under conditions of low conversion of isomerization, CTC is the charge-transfer complex between sulfur dioxide and the *cis*-2-butene molecule, and P<sub>b</sub> and P<sub>s</sub> represent the terminal group of 2-butyl and sulfonyl radical of a living polysulfone, respectively. The specific *cis-trans* isomerization proceeds via the addition and elimination of 2-butene molecules at the terminal of the polymer formed in the adsorption layer:



The geometrical isomerization on alkali and alkaline earth zeolites exhibited an acceleration of its rate with reaction time,

which can be attributed to a radical-type mechanism suggested above. It should be noticed that the formation of polysulfone

has been confirmed for  $\text{MnO}_2$  and  $\text{PbO}_2$  (8), but an attempt to find the production of polysulfone for  $\text{NaX}$ ,  $\text{CaX}$ , and  $\text{ZnX}$  zeolites by measuring pressure drop of reactants or by infrared spectroscopy has been unsuccessful. Förster and Seelemann also reported the absence of polysulfone for  $\text{NaA}$  and  $\text{NaCaA}$  zeolites by infrared spectroscopic observation, but suggested the formation of complex between  $\text{SO}_2$  and butene which has a sulfone-like structure (11). These results imply that formation of a long-chain polymer is inhibited in the narrow pores of zeolite. We believe that a very low-molecular-weight cooligomer of  $\text{SO}_2$  and butene would participate in the reaction. The decrease in the rate of geometrical isomerization with a rise in the amount of  $\text{SO}_2$  under high concentration of  $\text{SO}_2$  for  $\text{NaX}$ ,  $\text{MgX}$ , and  $\text{LaX}$  can be ascribed to an interference of the diffusion of butene molecules by the formed cooligomer in the narrow pores of zeolites as suggested previously (7). However, this does not exert any effect on the rates of double-bond migration for these zeolites because they are slower by a factor of 2 or 3 than those of geometrical isomerization.

The rapid reduction in the rate of geometrical isomerization with reaction time for rare earth zeolites (Figs. 5 and 6) might be attributed to the decrease in the number of living oligomers necessary for the isomerization because of a rapid consumption of adsorbed  $\text{SO}_2$  through the cooligomerization with butenes. This assumption is supported by the observation that the reduction is relaxed as the concentration of  $\text{SO}_2$  increases. In addition to this, accumulation of the formed oligomer with time might inhibit the reaction. These effects, rapid consumption of  $\text{SO}_2$ , and blocking of the oligomer can be neglected for alkali or alkaline earth zeolites with low concentrations of  $\text{SO}_2$  since the activities of these catalysts are low or moderate compared to those of the rare earth zeolites. Thus, the geometrical isomerization induced by  $\text{SO}_2$  for all the zeolites examined in this work can be explained by means of the polysulfone-accompanying mechanism proposed previously [Eqs. (1) to (8)] (7-9).

According to the reaction mechanism [Eqs. (1)-(8)] the initial rate of *trans*-2-butene formation can be expressed by either of the following two equations:

$$R_{c \rightarrow t}^0 = k_5 \left\{ \frac{k_2'(k_7 + k_4[\textit{cis-But}])}{k_8'(k_5 + k_6 + k_3[\text{SO}_2])} \right\}^{\frac{1}{2}} K[\textit{cis-But}][\text{SO}_2] \quad [\textit{initiation, (2)'; termination, (8'')}] \quad (9)$$

or

$$R_{c \rightarrow t}^0 = \frac{2k_2k_3K[\textit{cis-But}][\text{SO}_2]}{k_8 + k_8' \left\{ \frac{k_8/2 + k_5 + k_6 + k_3[\text{SO}_2]}{k_8'/2 + k_7 + k_4[\textit{cis-But}]} \right\}} \quad [\textit{initiation, (2); termination, (8) and (8')}] \quad (10)$$

Assuming that the adsorption sites are almost saturated by *cis*-2-butene under the pressure applied in this work ( $P_{\textit{cis-But}} \simeq 95$  Torr) and that at low concentration of  $\text{SO}_2$   $k_5 + k_6 \gg k_3[\text{SO}_2]$ , Eq. (9) will be

$$R_{c \rightarrow t}^0 = \frac{k_2'^{\frac{1}{2}}k_3}{k_8'} \left( \frac{k_7 + k_4\alpha}{k_5 + k_6} \right)^{\frac{1}{2}} K\alpha[\text{SO}_2], \quad (11)$$

where  $\alpha$  represents the concentration of adsorbed *cis*-2-butene saturated. It is reasonably assumed that  $k_8/2 \ll k_5 + k_6$  and  $k_8'/2 \ll k_7 + k_4\alpha$ ; then Eq. (10) will be

$$R_{c \rightarrow t}^0 = \frac{2k_2k_5(k_7 + k_4\alpha)K\alpha[\text{SO}_2]}{k_8(k_7 + k_4\alpha) + k_8'(k_5 + k_6)}. \quad (12)$$

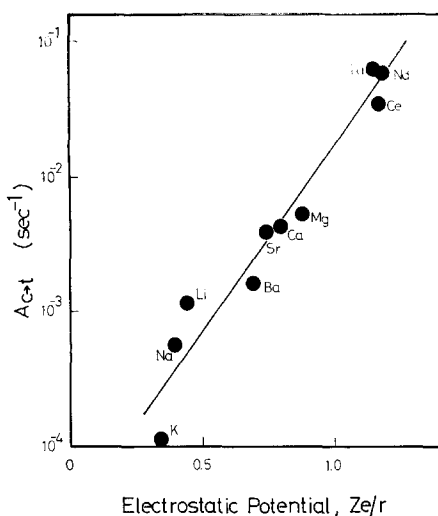


Fig. 10. Plot of  $A_{c \rightarrow t}$  as a function of electrostatic potential of cations of zeolites.

Experimental results that the rates are proportional to the amount of adsorbed SO<sub>2</sub> for alkali and alkaline earth zeolites are consistent with these equations.

It is reasonable to consider that the difference in activities among the catalysts results mainly from the difference in  $k_2$  which is the rate constant of the initiation step of the isomerization. Hence, the slopes of the plots in Figs. 2 and 5 indicate the activities of the alkali and alkaline earth zeolites for the initiation step of the reaction. In the case of rare earth zeolites, however, the rate of geometrical isomerization is not proportional to the amount of adsorbed SO<sub>2</sub> even at low concentrations of SO<sub>2</sub> (Figs. 7-9). This may be caused by the decrease in the amount of SO<sub>2</sub> effective in geometrical isomerization, because part of the preadsorbed SO<sub>2</sub> has been consumed through the reaction with basic  $\text{Re}(\text{OH})_2^+$  as will be discussed later. Hence, the maximum slopes at the point of inflection for the curves of  $R_{c \rightarrow t}^0$  versus the amount of preadsorbed SO<sub>2</sub> have been tentatively adopted as the activities for the rare earth zeolites.

It has been suggested in a previous study (9) that the SO<sub>2</sub>-2-butene charge-transfer

complex initiates *cis trans* isomerization. Let us hypothesize that the charge-transfer complex coordinated to the exposed metal cations of the cation-exchanged zeolites causes the initiation of the cooligomerization and, accordingly, of the geometrical isomerization under the influence of electrostatic field of the cations. As the sulfur dioxide in CTC is negatively charged because of a partial electron transfer from 2-butene, it must be the oxygen (negative) end of CTC that approaches to the positive metal ions. The activities of catalysts for the SO<sub>2</sub>-induced geometrical isomerization,  $A_{c \rightarrow t}(\text{SO}_2)$ , have been plotted as a function of electrostatic potential,  $Ze/r$ , or of electrostatic field strength of the cation of the zeolites in Figs. 10 and 11.  $Ze/r$  is the ionic charge divided by the effective ionic radius of the cation at the position of the oxygen atom, i.e., the sum of the radius of the metal cation and 1.40 Å (the latter is about the expected van der Waals radius of the oxygen atom), since we are concerned with an orbital on oxygen. The electrostatic field strength in the zeolites at the position of the oxygen atom of CTC was calculated from the data of Rabo *et al.* (12). These parameters are known as the measures of the polarizing power of a metal cation in its vicinity (13-19). Good correlations between the activity and the power of polarization or the field strength shown in Figs. 10 and 11 support the mechanism for the initiation step hypothesized above. The picture of the initiation process [Eq. (2)] that we have in mind is the polarization of the SO<sub>2</sub> of the CTC on metal cations, i.e., a transfer or moving away of both electrons in the lone-pair orbit of the oxygen atom away from the oxygen under the influence of the electrostatic field, and a consequent transfer of electrons from the sulfur toward the oxygen atom resulting in a strong polarization of CTC. An ion-radical transformed from this polarized CTC must initiate the reaction.



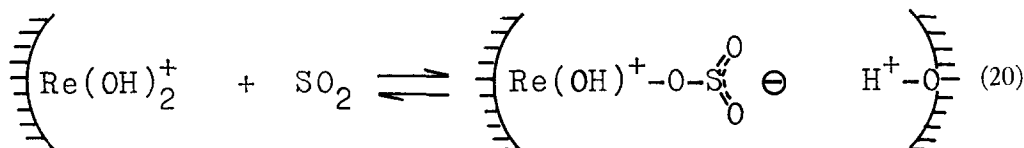
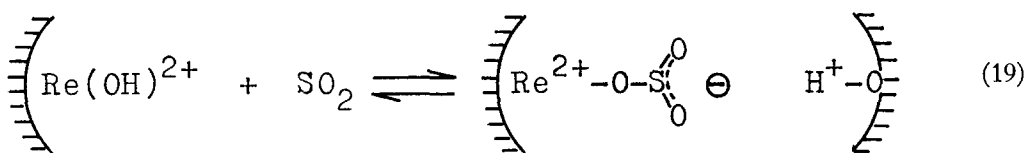


TABLE 2  
Activities of the Zeolites for SO<sub>2</sub>-Induced Double-Bond  
Migration of *cis*-2-Butene at 25°C

	Zeolite						
	BaX	SrX	CaX	MgX	NdX	CeX	LaX
Activity <sup>a</sup> (10 <sup>-4</sup> ·sec <sup>-1</sup> )	0.075	3.70	2.18	0.133	15.3	17.5	15.1

<sup>a</sup> See text.

For rare earth zeolites



where the hydrogen atoms of basic hydroxyl groups are transferred to zeolitic oxygen atoms. Assuming that the double-bond migration has been induced by these newly created OH groups, the rate of SO<sub>2</sub>-induced reaction for alkaline earth zeolites can be expressed as follows:

$$R_{c \rightarrow 1}^0 \propto [\text{H}_{\text{new}}^+] \quad (21)$$

$$[\text{H}_{\text{new}}^+] = K_{18}[\text{M}(\text{OH})^+][\text{SO}_2] \quad (22)$$

where,  $K_{18}$  is the equilibrium constant for reaction (18). Equation (21) explains the experimental result that  $R_{c \rightarrow 1}^0$  is proportional to the amount of SO<sub>2</sub> in its low concentration range. Thus, the slopes of the linear portion of the curves for the double-bond migration in Figs. 4a-d at the low concentrations of SO<sub>2</sub> indicate the relative activities of the zeolites which are proportional to  $K_{18}[\text{M}(\text{OH})^+]$  in Eq. (22). In the case of rare earth zeolites, the

activities were calculated from the dotted lines in Figs. 7-9. The values are summarized in Table 2.

The high catalytic activities for rare earth zeolites compared to alkaline earth zeolites might be attributed to the production of  $\text{Re}(\text{OH})_2^+$ , which has greater basicity than  $\text{M}(\text{OH})^+$ . The catalytic inactivity for alkali zeolites can be ascribed to a negligible dissociation of coordinated water due to the weak polarizing ability of alkali cations.

#### ACKNOWLEDGMENTS

The authors wish to express their appreciation to Mr. Kiyoshi Eshima for valuable assistance during the experimental work.

#### REFERENCES

1. Minachev, Kh. M., and Isakov, Ya. I., *Advan. Chem. Ser.* 121, 451 (1973).
2. Jacobs, P. A., "Carboniogenic Activity of Zeolites." Elsevier/North-Holland, Inc., New York, 1977.

3. Kolenikov, I. M., *Russ. Chem. Rev.* **44**, 306 (1975).
4. Miale, J. N., and Weisz, P. B., U.S. Patent 3,175,967; *Chem. Abstr.* **63**, 12947b (1965).
5. Miale, J. N., and Weisz, P. B., U.S. Patent 3,240,697; *Chem. Abstr.* **64**, 15054e (1966).
6. Otsuka, K., and Morikawa, A., *J. Chem. Soc. Chem. Commun.* **1975**, 218.
7. Otsuka, K., and Morikawa, A., *J. Catal.* **46**, 71 (1977).
8. Otsuka, K., Tanabe, T., and Morikawa, A., *J. Catal.* **48**, 333 (1977).
9. Otsuka, K., Eshima, K., and Morikawa, A., *Bull. Chem. Soc. Japan* **50**, 631 (1977).
10. Otsuka, K., Oouchi, R., and Morikawa, A., *J. Catal.* **50**, 379 (1977).
11. Forster, H., and Seelemann, R., *J. Chem. Soc. Chem. Commun.* **1976**, 1060.
12. Rabo, J. A., Angell, C. L., Kasai, P. H., and Schomaker, V., *Discuss. Faraday Soc.* **41**, 328 (1966).
13. Hirschler, A. E., *J. Catal.* **2**, 428 (1963).
14. Richardson, J. T., *J. Catal.* **9**, 182 (1967); **11**, 275 (1968).
15. Pickert, P. E., Rabo, J. A., Dempsey, E., and Schomaker, V., in "Proceedings, 3rd International Congress on Catalysis, Amsterdam, 1964," Vol. 1, p. 714. Wiley, New York, 1965.
16. Angell, C. L., and Schaffer, P. C., *J. Phys. Chem.* **70**, 1413 (1966).
17. Angell, C. L., and Howell, M. V., *J. Phys. Chem.* **73**, 2551 (1969).
18. Ward, J. W., *J. Catal.* **10**, 34 (1968).
19. Sugihara, H., Shimokoshi, K., and Yasumori, I., *J. Phys. Chem.* **81**, 669 (1977).
20. Foster, N. F., and Cvetanovic, R. J., *J. Amer. Chem. Soc.* **82**, 4274 (1960).
21. Hightower, J. W., and Hall, W. K., *J. Catal.* **5**, 99 (1966).
22. Ward, J. W., *J. Phys. Chem.* **72**, 2689, 4211 (1968).
23. Christner, L. G., Liengme, B. V., and Hall, W. K., *Trans. Faraday Soc.* **64**, 1679 (1968).
24. Uytterhoeven, J. B., Schoonheydt, R., Liengme, B. V., and Hall, W. K., *J. Catal.* **13**, 425 (1969).
25. Ward, J. W., *J. Catal.* **10**, 34 (1968).
26. Moscou, L., *Advan. Chem. Ser.* **102**, 250 (1971).
27. Moscou, L., and Lakeman, M., *J. Catal.* **16**, 173 (1970).
28. Nakata, K., Otsuka, K., and Morikawa, A., unpublished data.
29. Mirodatos, C., Pichat, P., and Barthomeuf, D., *J. Phys. Chem.* **80**, 1335 (1976).
30. Mirodatos, C., Kais, A. A., Vedrine, J. C., Pichat, P., and Barthomeuf, D., *J. Phys. Chem.* **80**, 2366 (1976).